Methods of machine learning and stochastic modeling for the structural characterization of functional battery materials at various length scales

P. Rieder[1], O. Furat[1], P. Weddle[2], J. Allen[2], D.P. Finegan[2], K. Smith[2], V. Schmidt[1]

[1]Institute of Stochastics, Ulm University, Ulm, Germany, [2]National Renewable Energy Laboratory, Golden (Colorado), USA

MOTIVATION & WORKFLOW

- **SEM, nano CT** and **FIB-EBSD** provide detailed 2D and 3D image data of nano- and microstructures of functional materials
- Cost for 3D imaging and insufficient information provided by 2D imaging for investigating descriptors related to transport paths **motivates the development** of a stochastic 3D crack model to address this stereological challenge.
- Utilize **spatial stochastic modeling** for the **holistic structural characterization** of active material (AM) particles in Li-ion battery electrodes
  - Allows generation of arbitrarily many **virtual, but realist** cracked AM particles
  - Realizations can serve as **input** for several **numerical simulations**
- Investigation of **3D structure-property relationships**, i.e., how effective material properties are influenced by their nano- and microstructure
- Provide **structuring recommendations** for manufacturing processes of optimized battery materials

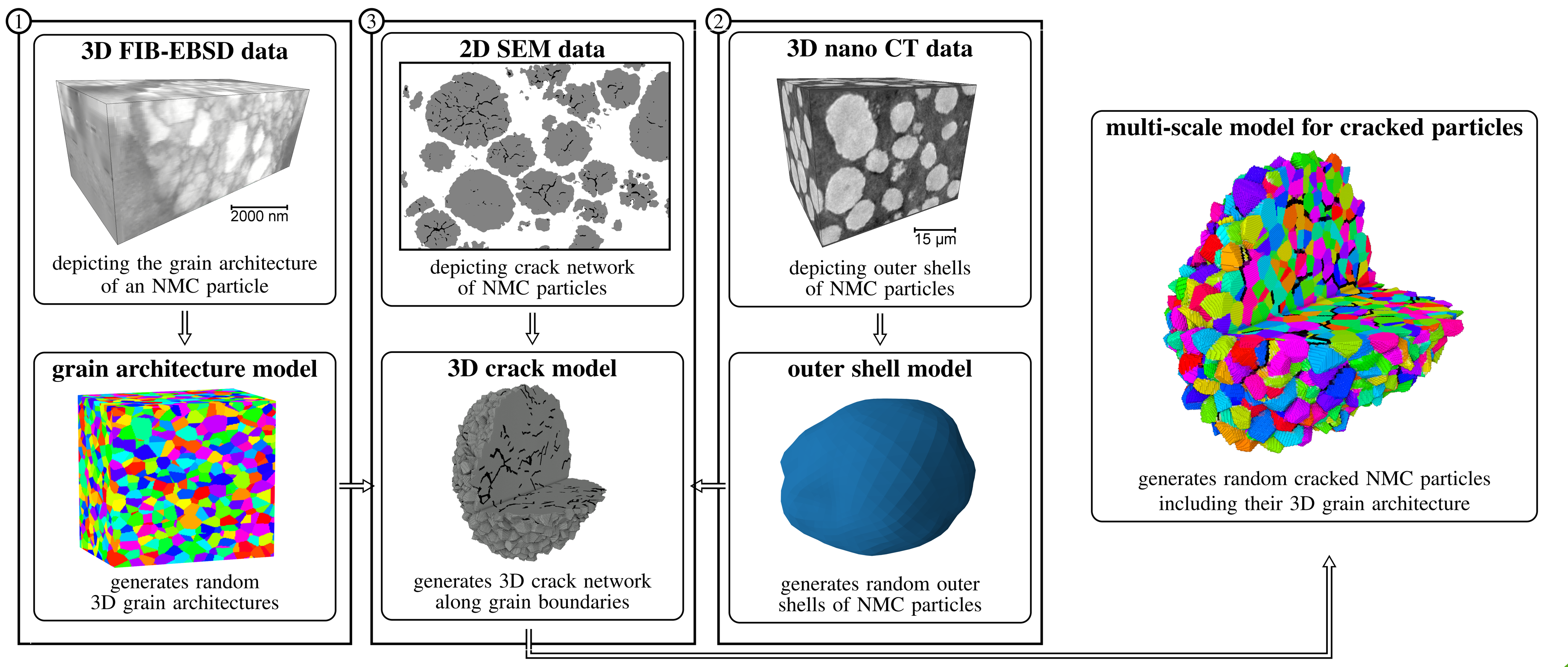

1. GRAIN ARCHITECTURE

Image segmentation using a convolutional neural network

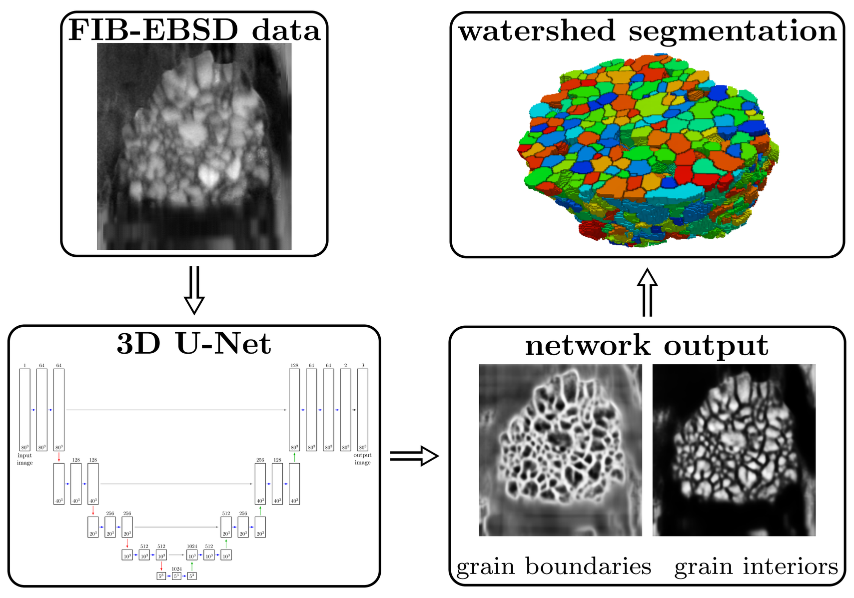

A 3D U-Net [1] was trained to enhance grain boundaries in FIB-EBSD data. Then, a grain-wise segmentation is computed, utilizing a marker-based watershed algorithm [2].

Grain architecture model

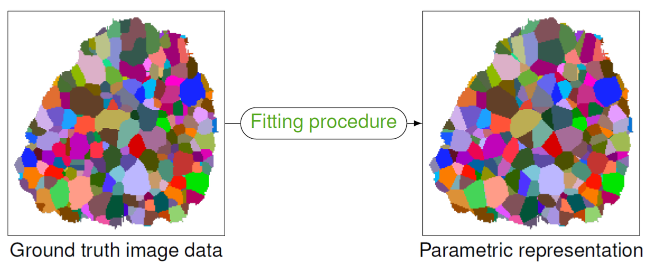

Parametric representation $\{(y_i, r_i)\}_{i=1}^n \subset \mathbb{R}^4$ of segmented 3D EBSD data by Laguerre tessellation is determined [3]. The i-th cell of the tessellation is given by

$$C_i = \{x \in \mathbb{R}^3 \colon |x - y_i|^2 - r_i \leq |x - y_j|^2 - r_j \text{ for all } i \neq j\}.$$

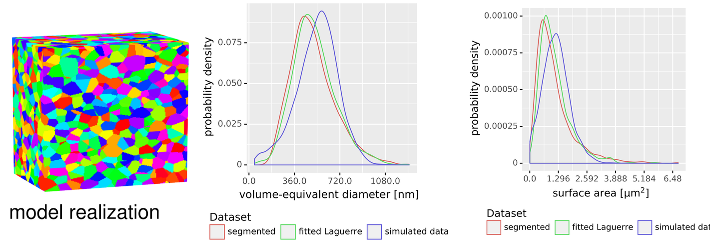

The grain architecture model is derived by fitting a stochastic model to the marked point pattern $\{(y_i, r_i)\}_{i=1}^n$ [4].

2. OUTER SHELL

Outer shell model

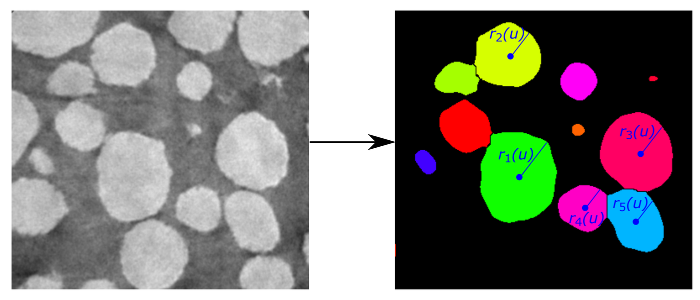

Nano-CT data of NMC particles is segmented [4]. Particles are represented by radius functions $r_1, \ldots, r_n$: $S^2 = \{x \in \mathbb{R}^3 \colon \|x\| = 1\} \to [0, \infty)$.

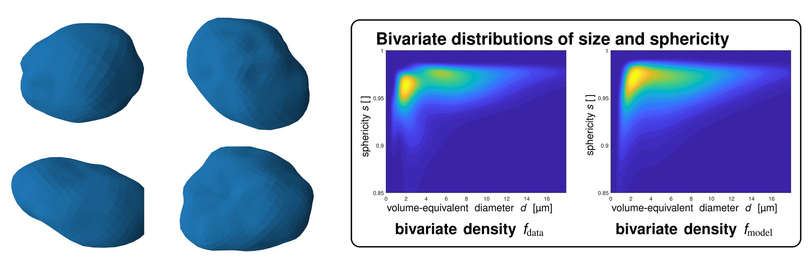

Isotropic Gaussian fields R (on the sphere) can be used to model radius functions [4]. The parameters of a mixture of Gaussian fields are fitted to $r_1, \ldots, r_n$.

1.+2. PRISTINE MODEL

Multi-scale pristine model

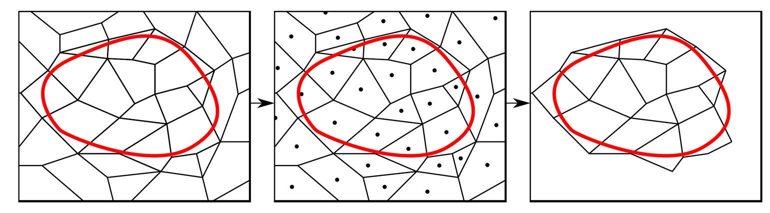

Left: Realization of the grain architecture and outer shell. Center: Centers of mass for each grain. Right: Deletion of grains whose centers are not in the outer shell.

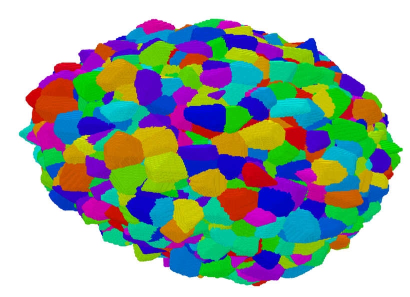

Multi-scale model for pristine particles [4]

(i) characterizes the shape of particles,
(ii) characterizes the grain architecture of particles,
(iii) can be used to generate input for numerical simulations [5].

3. CRACK NETWORK

Crack segmentation

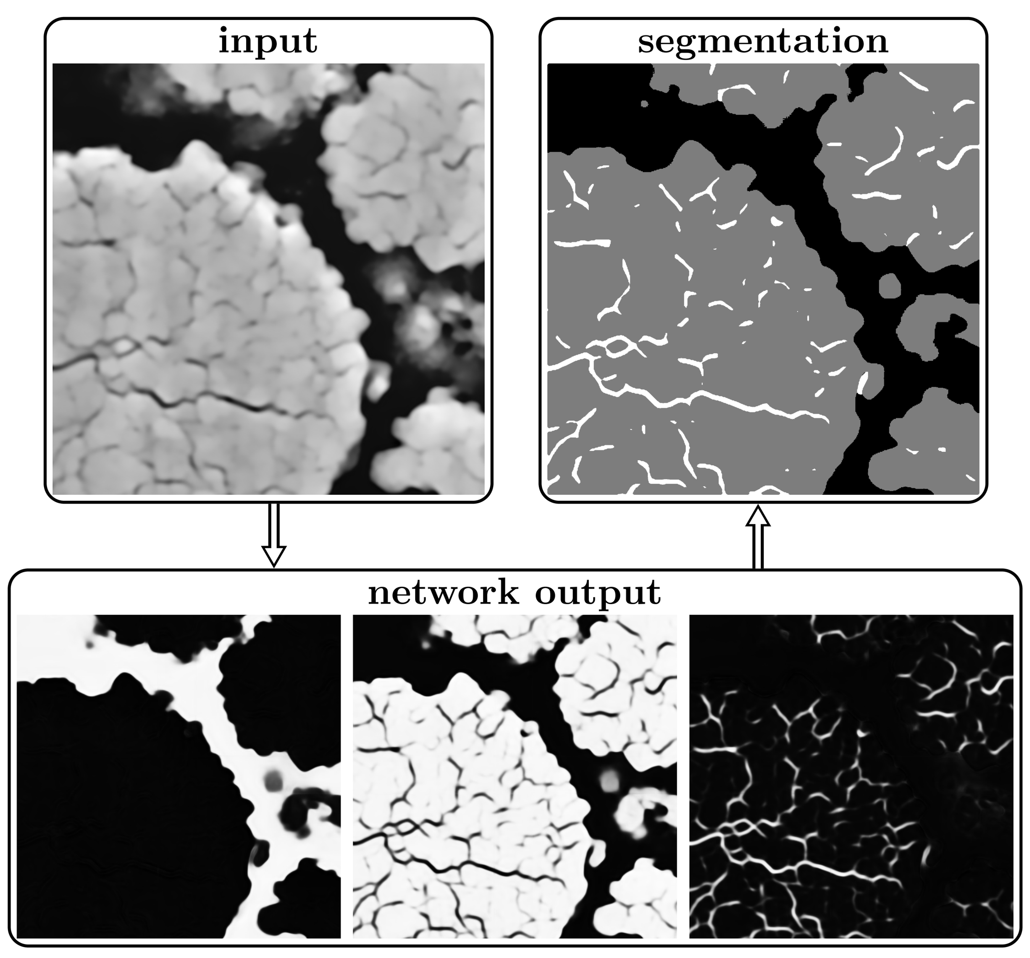

A U-net [6] is trained to segment (super-resolved [7]) SEM images into background, cracks and solid phase .

Stochastic 3D crack model

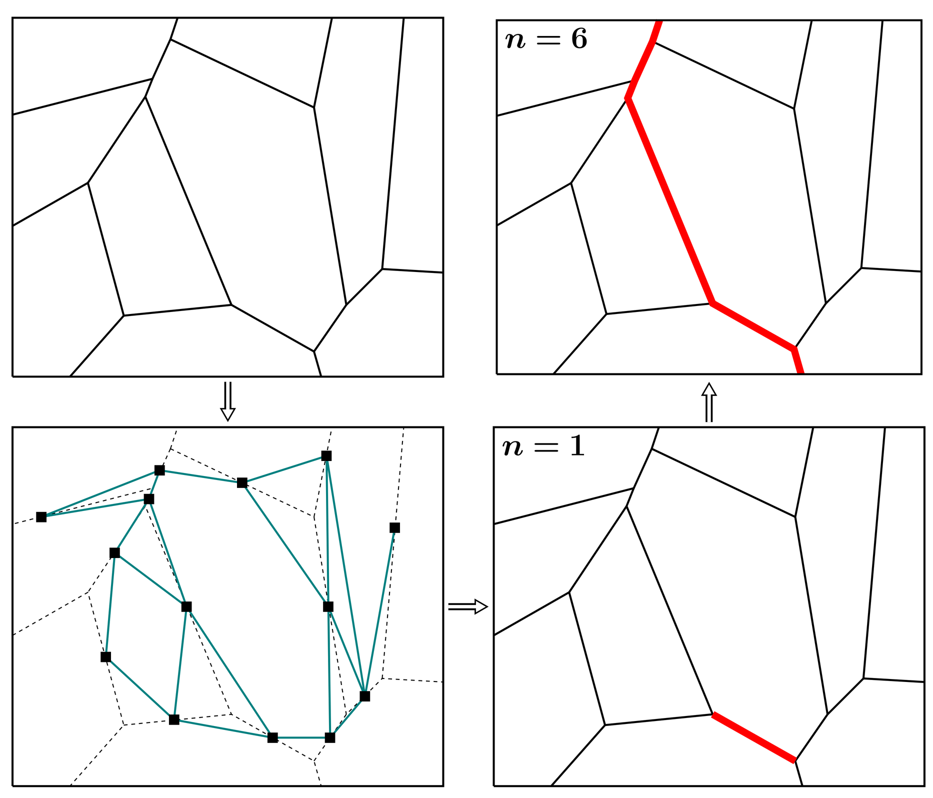

The grain architecture is represented as adjacency graph of grain boundaries (facets). A crack is modeled by choosing an initial facet followed by iteratively adding neighboring facets, based on their alignment w.r.t. the priorly chosen facet path [8]. Finally, the chosen facets are dilated to model the crack.

Calibration and validation

The parameters of the 3D crack model are fitted by minimizing a loss function, which measures the discrepancy between virtual 2D cross sections with 2D SEM data [8].

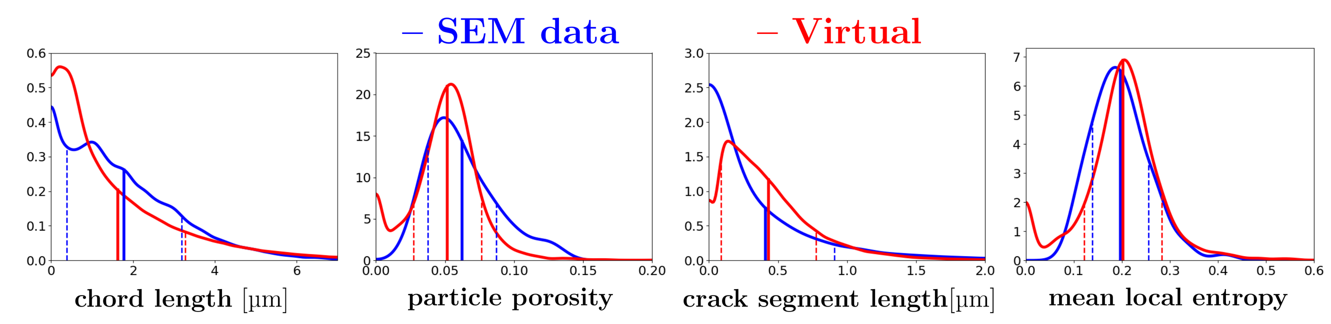

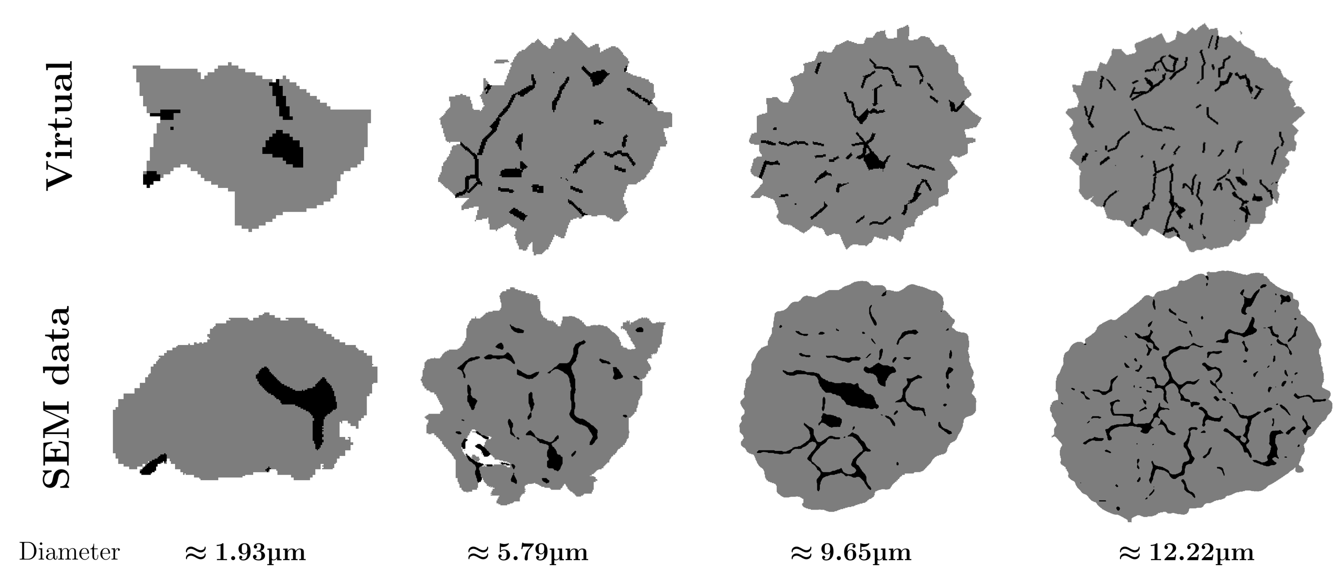

REFERENCES

[1] O. Çiçek, A. Abdulkadir, S. S. Lienkamp, T. Brox, O. Ronneberger. 3D U-Net: Learning dense volumetric segmentation from sparse annotation. Lecture Notes in Computer Science, vol 9901. Springer (2016), 424-432.

[2] O. Furat, D.P. Finegan, D. Diercks, F. Usseglio-Viretta, K. Smith, V. Schmidt, Mapping the architecture of single electrode particles in 3D, using electron backscatter diffraction and machine learning segmentation. J. Power Sources 483 (2021), 229148.

[3] L. Petrich, O. Furat, M.Y. Wang, C.E. Krill III, V. Schmidt, Efficient fitting of 3D tessellations to curved polycrystalline grain boundaries. Frontiers in Materials 8 (2021), 60602.

[4] O. Furat, L. Petrich, D.P. Finegan, D. Diercks, F. Usseglio-Viretta, K. Smith, V. Schmidt, Artificial generation of representative single Li-ion electrode particle architectures from microscopy data. npj Comput. Mater. 7 (2021), 105.

[5] J. Allen, P.J. Weddle, A. Verma, A. Mallarapu, F. Usseglio-Viretta, D.P. Finegan, A. Colclasure, W. Mai, V. Schmidt, O. Furat, D. Diercks, T. Tanim, K. Smith, Quantifying the influence of charge rate and cathode-particle architectures on degradation of Li-ion cells through 3D continuum-level damage models, J. Power Sources 512 (2021), 230415.

[6] O. Ronneberger, P. Fischer, T. Brox, U-Net: Convolutional networks for biomedical image segmentation. In *Proceedings of Medical Image Computing and Computer-Assisted Intervention*, (Cham, Switzerland, 2015), pp. 234–241.

[7] O. Furat, D.P. Finegan, Z. Yang, T. Kirstein, K. Smith, V. Schmidt, Super-resolving microscopy images of Li-ion electrodes for fine-feature quantification using generative adversarial networks. npj Comput. Mater. 8 (2022), 68.

[8] P. Rieder, O. Furat, F. Usseglio-Viretta, J. Allen, P. Weddle, D. P. Finegan, K. Smith, V. Schmidt, 2024, Stochastic 3D reconstruction of cracked polycrystalline NMC particles using 2D SEM data, working paper.

Download the poster

Contact: Philipp Rieder, philipp.rieder@uni-ulm.de, +49(0) 731 50 23525, Institute of Stochastics, Ulm University

EFFECTIVE PROPERTIES

Transport path lengths (ion transport)

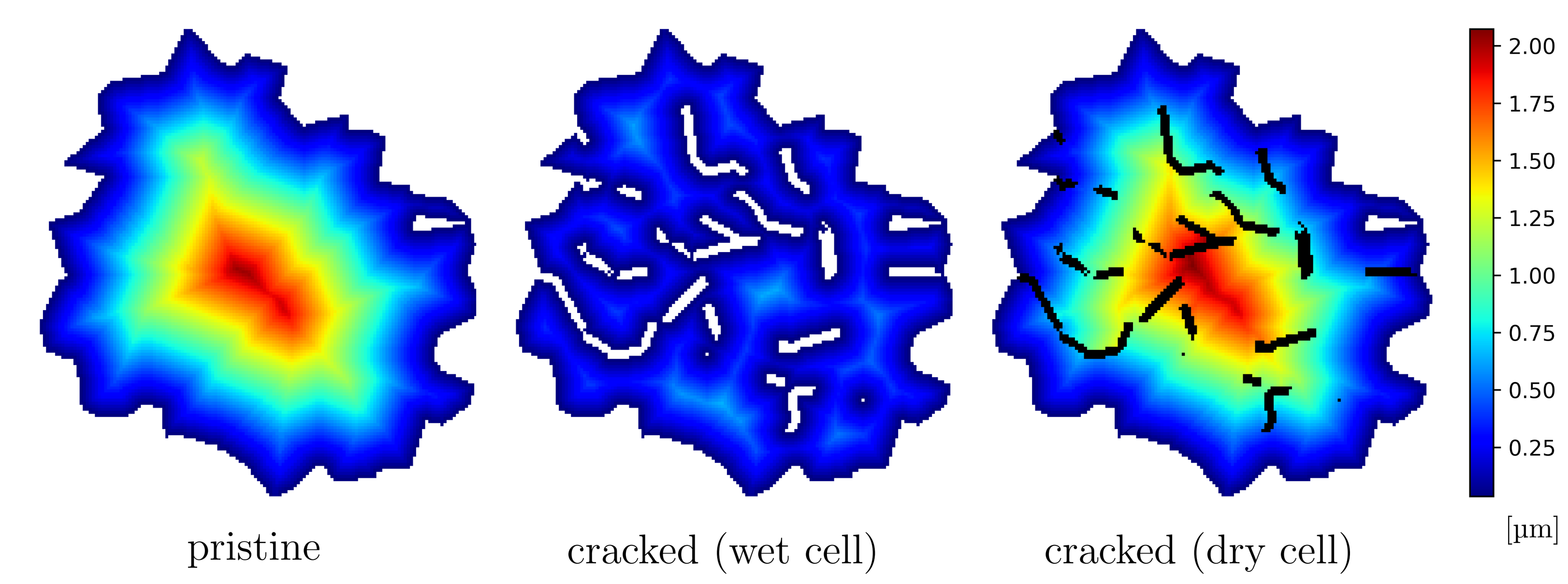

Realizations of the stochastic 3D for cracked particles can be utilized to investigate the change of path lengths before (left) and after cracking. The change of path lengths for ion transport depends on the kind of battery. In wet cell batteries, cracks are flooded with electrolyte, resulting in shorter paths (middle). Conversely, in dry cell batteries, cracks typically serve as obstacles, leading to an increase in path lengths (right).